Probing the association between resting state brain network dynamics and psychological resilience

Dominik Kraft[1], Christian J. Fiebach[1,2]

[1] Department of Psychology, Goethe University Frankfurt, Germany

[2] Brain Imaging Center, Goethe University Frankfurt, Frankfurt am Main, Germany

Total number of words: 6545 (excluding tables, figures, and references)

Address for Correspondence:

Dominik Kraft
Department of Psychology, Goethe University Frankfurt, Theodor-W.-Adorno-Platz 6, Frankfurt am Main 60323, Germany
Electronic address: dominik.kraft@gmail.com

Supplementary File 1:

- fMRI preprocessing details
- Correlational results on the nodal level without covariates (Figure S1, S2)

Abstract

This study aimed at replicating a previously reported negative correlation between node flexibility and psychological resilience. To this end, we acquired multiband resting-state BOLD fMRI (TR = .675 sec) from 60 participants and assessed resilience with three psychological questionnaires. Time resolved functional connectivity was calculated by performing a sliding window approach on averaged time series from the Schaefer 100 parcellation, resulting in 753 connectivity matrices. Node degree was calculated as a proxy for time-varying connectivity. Multilayer modularity detection was performed to track network reconfigurations over time and to calculate node flexibility (the number of times a node changes community assignment) and node promiscuity (the fraction of communities a node participates in). We found no significant correlations between resilience and any of the measures of dynamic functional connectivity, neither at nodal, functional network, or global levels. Results were also robust against down-sampling the data to resemble a conventional TR of ~2 sec (as in the original study) and against the application of different windowing schemes (overlapping vs. non-overlapping, different window lengths). We discuss several methodological reasons that may account for the difference in results between the present and the original study, to inform future network neuroscience studies of mental health.

Author Summary

We tested the replicability and generalizability of a previously proposed negative association between dynamic brain network reconfigurations derived from multilayer modularity detection and psychological resilience. Using temporally more highly resolved resting-state BOLD fMRI data and analyzing several measures of brain network dynamics (node flexibility, node promiscuity, nodal degree) we could however not establish any significant correlations between psychological resilience and dynamic functional connectivity. Our findings were robust against changes in the sampling (i.e., after down-sampling the time series) and sliding window scheme (overlapping vs. non-overlapping, window length). We conclude that further research is needed to understand the network neuroscience basis of mental health and discuss several reasons that may account for the variability in results.

Technical Terms:

Multilayer modularity detection:
- detection of highly connected nodes (i.e., modules) in temporal, ordinal networks

Time varying functional connectivity:
- functional connectivity that varies over time, often labeled as 'dynamic connectivity'

Functional connectivity:
- statistical dependencies among (fMRI) time series from different regions, nodes, or networks

Sliding window correlation:
- FC calculation over a defined window, which is shorter than the whole time series. Window type may vary in its appearance. Sliding the window over the time series can produce time resolved functional connectivity (one matrix per window)

Multiband EPI
- Fast echo planar imaging (EPI) sequence which is characterized by the simultaneous acquisition of multiple slices. Multiband EPI shortens the acquisition time of a single brain volume and thus allows to acquire more data at a given time.

Down-sampling:
- Creating a 'slower' i.e., less densely sampled time series by artificially selecting every x^{th} timepoint

Graph Theory:
- Mathematical tool to model and analyze pairwise relations between different objects (here: timeseries from brain regions and their functional connectivity)

keywords:

resting state – time varying connectivity – multilayer modularity – psychological resilience – network reconfigurations – node flexibility – node promiscuity – node degree

Introduction

Abundant literature in human clinical neuroscience has established a link between changes in intrinsic functional connectivity of large-scale brain networks and psychological disorders such as depression (Mulders et al., 2015) or schizophrenia (Dong et al., 2018; see also Menon, 2011 for a general overview). As a consequence, researchers have started to explore also whether differences in functional network architecture contribute to individual differences in preserving mental health in the face of stress and adversity (resilience; e.g., Southwick & Charney, 2012). Two recent studies (Long et al., 2019; Paban et al., 2019) have reported associations between psychological resilience and brain network dynamics using multilayer modularity, a relatively new tool from the evolving field of network neuroscience that integrates spatial and temporal information (Muldoon & Bassett, 2016). In both studies, psychological resilience was assessed with a frequently-used questionnaire measure, the Connor-Davidson Resilience Scale (CD-RISC; Connor & Davidson, 2003), and network dynamics under task-free (resting-state) conditions were examined by detecting time-evolving patterns of non-overlapping and coherent modules and by quantifying the frequency with which brain nodes switched between modules (*node flexibility;* Bassett et al., 2011).

Paban et al. (2019) measured EEG under task-free conditions and conducted network analyses in source space. Negative correlations between node flexibility and resilience were observed in the alpha, beta, and delta frequency bands, including 'rich club' areas like the superior parietal cortex, medial orbitofrontal cortex, and cuneus. This may appear counterintuitive at first glance, as more flexible networks appear to be better able to adapt to changing demands or adversity. However, the authors argue that more stable brain networks may be associated with resilience because they prevent from excessive reconfigurations following external stressors or adversity. A subsequent resting state functional MRI (rs-fMRI) study (Long et al., 2019) also reports lower node flexibility in more resilient persons, primarily in visual cortices and the left medial-orbital portion of the superior frontal gyrus. Across both studies, there exists a partial overlap with regard to a visual region, the lingual gyrus. However, beyond visual areas, localization results also differed between studies and Long et al. (2019) did not replicate correlations between resilience and node-level flexibility in 'higher order' (e.g., superior parietal, inferior frontal) brain areas (Paban et al., 2019).

Some of these inconsistencies may result from inherent differences between measurement modalities (e.g., the substantial difference in the temporal resolution of ‘standard’ fMRI and EEG) whereas others may reflect specific methodological choices by the authors. For example, the fMRI ‘dynamics’ studied by Long et al. (2019) involved only a timeseries of 12 non-overlapping time windows (each of 20 sample points length, derived from 250 measurements of TR = 2 sec). Even though a gold standard for data length for analyses of dynamic multilayer modularity is yet to be established, recent studies suggest that more data are required for sensitive and reliable estimation of network dynamics from BOLD fMRI (Hindriks et al., 2016; Lurie et al., 2020; Yang et al., 2021). To ameliorate such potential methodological shortcomings and to further our understanding of the relationship between resilience and brain network dynamics, we aimed at replicating and extending these results using temporally more highly resolved resting state BOLD data (multiband sequence; MB factor 4; TR = .675 sec). 52 healthy young adults completed three different resilience questionnaires, and multilayer modularity analyses were conducted based on a timeseries of 753 overlapping windows derived using a sliding window approach (Figure 1). Node flexibility was calculated as the number of times a node changes its community assignment between windows, divided by the total possible number of changes (Bassett et al., 2011). Given the results of Long et al. (2019), we expected that subjectively rated resilience and node flexibility should be negatively correlated.

To extend previous work and to provide a more complete characterization of the relationship between dynamic network connectivity and resilience, we also assessed node promiscuity (i.e., the fraction of communities a node participates in at least once, across all layers (Papadopoulos et al., 2016), and node degree, the binary sum of dynamic connections for each node, whereby connections are only considered as ‘dynamic’ if the standard deviation of their correlations with other nodes over time differs significantly from surrogate data (which represent a 'static', i.e., time invariant, null model; Savva et al., 2019). All analyses were conducted at nodal and global levels (using average measures across nodes), as well as independently for seven functionally defined resting state networks (RSN, Yeo et al., 2011). Lastly, we replicated all analyses in down-sampled data and with non-overlapping windows, to more directly compare our results to those of Long and colleagues (2019).

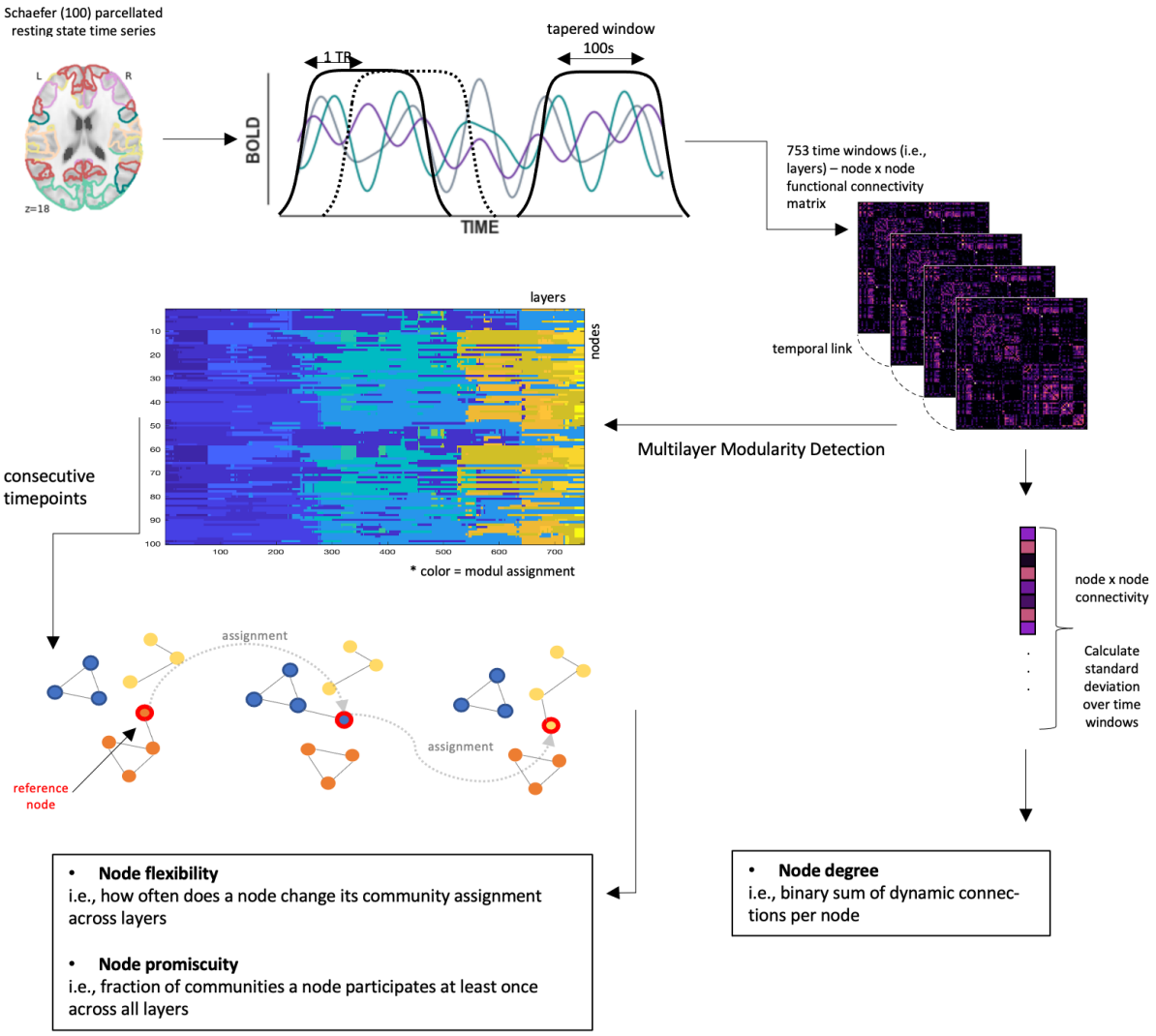

Figure 1. Schematic illustration of the workflow. Starting with the mean resting state time series from 100 nodes, 753 functional connectivity matrices (layers) representing correlations between the 100 different nodes were calculated via a sliding-window approach (window size = 100 sec, offset = 1 TR). For each node x node connection, the standard deviation was calculated over time; multilayer modularity detection was performed on ordinal layers. Network measures were calculated as described in the figure; see Methods section for details.

Results

Behavioral Results: Subjective Resilience Ratings

Descriptive statistics for the three resilience scales can be obtained from Table 1. Psychometric properties of the three questionnaires were satisfactory, with internal consistencies (Cronbach's alpha) ranging between .7 and .85 (see Table 1). Resilience

scores in our sample were comparable to the empirical results from the respective original publications (German version of the CD-RISC: 30.6, Sarubin et al., 2015; German version of the RS-13: 70, Leppert et al., 2008; German version of the BRS: 3.58 and 3.37 in two different samples, Chmitorz et al., 2018). Subjective ratings on the three questionnaires were significantly intercorrelated in our sample: CDRISC – RS, $r = .60$; CDRISC – BRS, $r = .61$; BRS – RS, $r = .45$, all $p < .001$ (FDR-corrected for multiple comparisons).

Table1. Descriptive statistics of resilience questionnaires (N = 52)

	CDRISC	**RS**	**BRS**
M (*SD*)	28.88 (4.73)	71.37 (10.06)	3.72 (.73)
min – max	18 - 38	21 - 87	1.83 – 5.00
α (95% CI)	.70 (.56- .81)	.85 (.79- .91)	.82 (.73-.89)

Note: M = mean, SD = standard deviation, min = minimum, max = maximum, α = Cronbach's alpha, CI = confidence interval.

Dynamic network measures in original vs. down-sampled functional connectivity data

In the following, we will report all results from correlational analyses both for the original data (TR = .675 sec) and for a down-sampled version of the timeseries that is as close as possible to the data used in Long et al. (2019), i.e., down-sampled by a factor of 3, resulting in a temporal resolution of TR = 2.025 sec (see Methods for more details). Down-sampling shifted node flexibility and promiscuity metrics towards higher values. However, there was a high spatial similarity (i.e., correlation) between original and down-sampled data for nodal flexibility ($r = .95$, $p < .0001$) and for node promiscuity ($r = .93$, $p < .0001$). For node degree we observed a significantly lower nodal degree in the down-sampled data compared to the original data, $t(99) = 15.15$, $p < .0001$, which is consistent with a recent report by Pedersen et al. (2018) that fewer data result in lower nodal degree values. Of note, for the original data participants had between 0.12 – 0.75% ($M = 0.33$) significant connections after testing against surrogate data, whereas this range dropped to 0.06 – 0.61% for the down-sampled data ($M = 0.20$).

Given that no previous data exist to derive specific hypotheses for the relationship between most measures assessed here and resilience, all associations were tested using Spearman correlations.

Correlation between dynamic functional connectivity measures and resilience

For all correlation analyses, we included as covariates of no interest age, gender, and framewise displacement to resemble the analyses by Long et al. (2019; see Methods). We observed no significant correlations for any of the combinations between the three brain measures of global flexibility, global promiscuity, or global degree and the three resilience questionnaires, neither for the original data (-.07 < *r* < .11; all *p* > .89) nor for the down-sampled data (-.17 < *r* < .09; all *p* > .53). We also found no significant correlations between any of the three questionnaires and node flexibility, node promiscuity, or degree at the level of functional networks (RSN), neither for the original (-.30 < *r* < .23, all *p* > .24; Figure 2A) nor for the down-sampled data (-.31 < *r* < .27, all *p* > .17; Figure 2B).

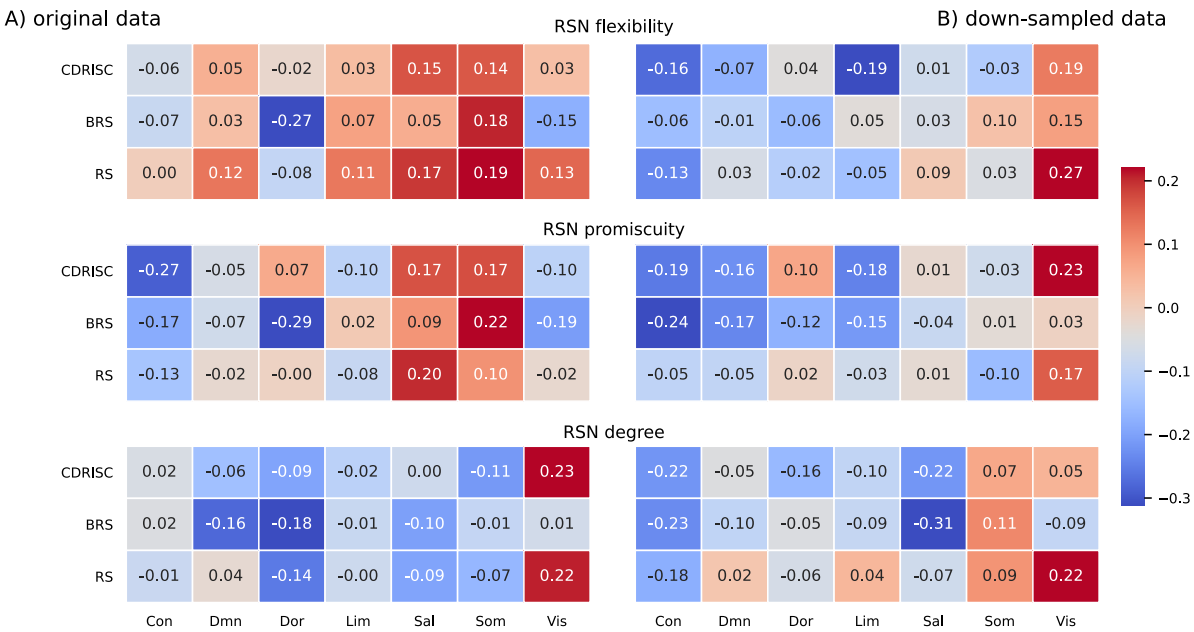

Figure 2. Correlations between network measures and resilience at the level of resting state networks (RSN) for the (A) original data (multiband; TR = .675 sec) and (B) down-sampled data (TR = 2.025 sec; see Methods for details). The number in each cell represents the respective correlation coefficient; all p > .17. Network labels: Con = frontoparietal-control, Sal = salience/ventral attention, Lim = limbic, Dor = dorsal attention, Som = somatomotor, DMN = default mode, Vis = visual. Resilience questionnaires: CDRISC = Connor-Davidson Resilience Scale, BRS = Brief Resilience Scale, RS = Resilience Scale.

Lastly, we also did not observe any significant correlations between resilience and the three network measures at the nodal level, neither for the original (-.41 < *r* < .46, all p

> .06; Figure 3) nor down-sampled data (-.32 < *r* < .33, all *p* > .69; Figure 4). Re-calculation of all node-level correlations without covariates yielded the same pattern of results (cf. Supplementary File 1, Figures S1 and S2): Data in original (MB) resolution yielded correlations in the range of -.47 < *r* < .42, all *p* > .1, except for the correlation between BRS and node promiscuity in one left dorsal attention network region (*r* = -.47, *p* = .05), which we however do not interpret as strong evidence as it is at the borderline of significance. For the down-sampled data, correlations were almost identical to the initial analysis with covariates (-.36 < *r* < .35, all *p* > .69).

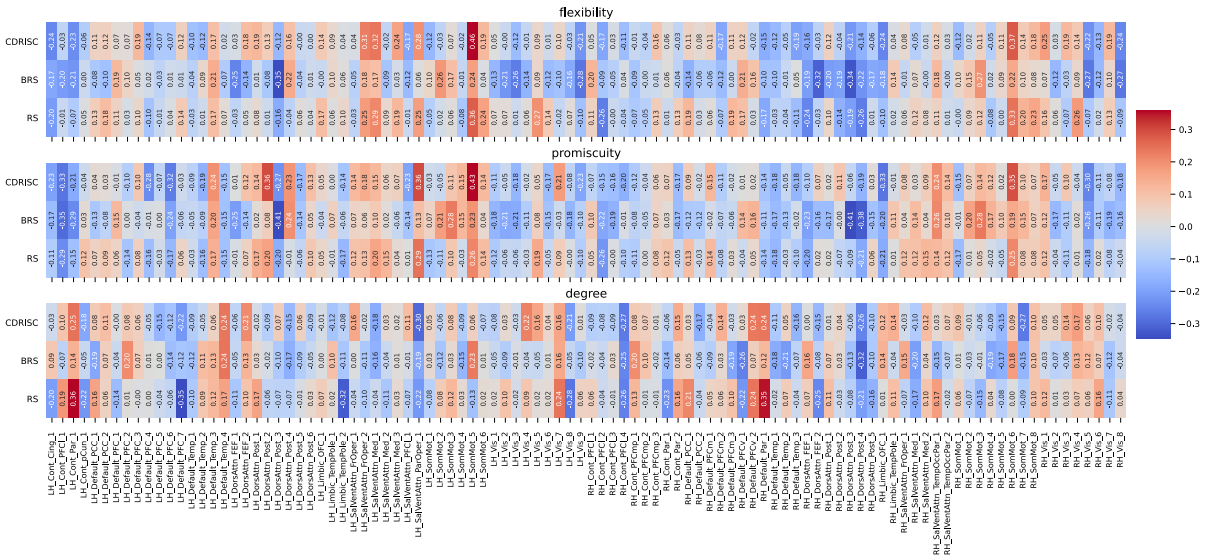

Figure 3. Correlations between network measures and resilience at the nodal level for the original (multiband) data (TR = .675 sec). Node names are depicted on the x-axis ticks; for a detailed list see https://bit.ly/3yvOBwz. LH = left hemisphere, RH = right hemisphere.

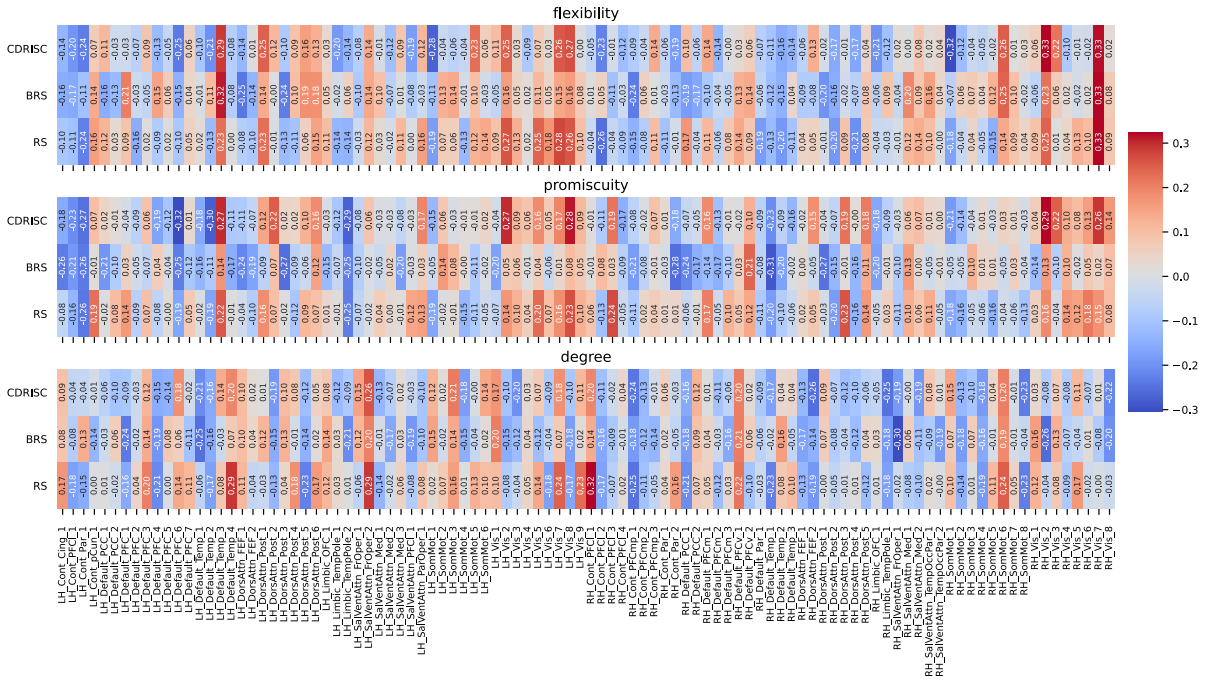

Figure 4. Correlations between network measures and resilience at the nodal level for the down-sampled data (TR = 2.025 sec). Node names are depicted on the x-axis ticks; for a detailed list see https://bit.ly/3yvOBwz. LH = left hemisphere, RH = right hemisphere.

Effects of overlapping vs. non overlapping time windows.

The above-reported analyses with down-sample BOLD data differ in one major aspect from those reported by Long et al. (2019), i.e., by the fact that we analyzed a high number of overlapping time windows (i.e., 753 in the original resolution and 251 in the down-sampled data) whereas Long et al. (2019) segmented their data into 12 non-overlapping time windows. When resolving our down-sampled data with a non-overlapping window scheme of length 20 TR as in the original study (in our data resulting in 15 windows), we did observe quantitative changes in nodal flexibility, i.e., flexibility values were scaled by a factor of approx. 10 (compare the y axis scaling of Figures 5A and 5B). However, we also observed that a high spatial similarity was preserved between node flexibility derived from down-sampled data with overlapping vs. non-overlapping windows (r = .93, p < .0001; Figure 5C,D), indicating no qualitative differences between both window schemes. Consistent with this, we also did not observe any correlations between node flexibility and self-reported resilience using this alternative approach (all p > .27, except for two correlations between BRS and node flexibility in right somatomotor network regions (both r = .44, p = .05), which we however do not interpret as strong evidence as it is at the border of significance.

Effects of window length.

To further explore whether and how node flexibility changes as a function of window length in the original data, we calculated node flexibility values for different window lengths between 40 and 100 sec in steps of 20. Similarly, to the effect of down-sampling the time series, we observed an increase in node flexibility with decreasing window size (Figure 5E), however with a high spatial similarity between flexibility values, i.e., all $r > .88$, $p < .0001$ (see Figure 5F). Similar to our initial analysis, we did not observe any significant correlations between node flexibility and resilience when varying the window size between 40 and 80 sec (all $p > .43$, except for one correlation between the CD-RISC and node flexibility in one region of the default mode network ($r = 47$, $p = .05$), derived from a window size of 80 sec.

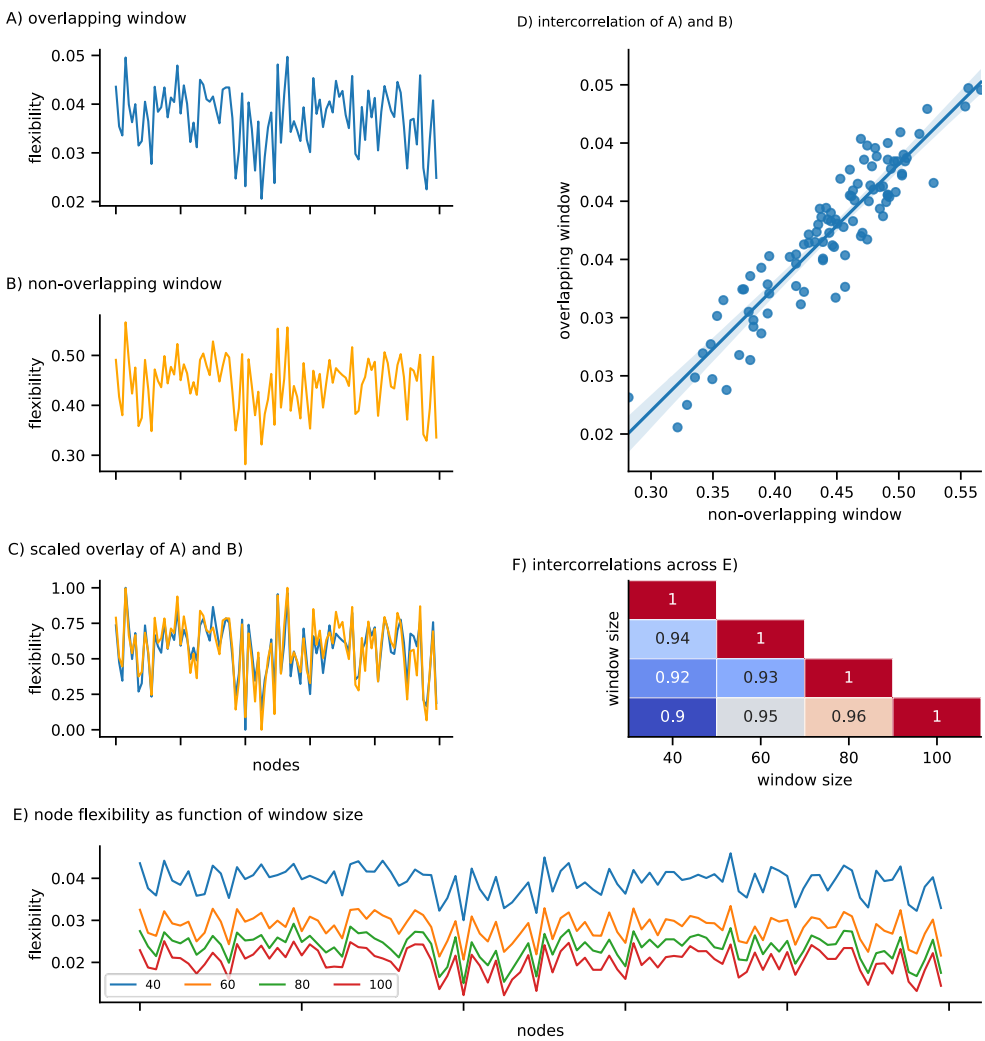

Figure 5. Influence of methodological differences in dynamic network analysis on node flexibility. Node flexibility for the down-sampled data (TR = 2.025 sec) with (A) overlapping (window size = 50TR) vs (B) non overlapping windows (window size = 20TR). Overlaying rescaled variants of both

arrays indicates (C) only minor differences between node flexibility values derived from different window schemes and d) high spatial similarity, i.e., a high correlation coefficient, between (A) and (B). (E) Node flexibility for the original data (multiband, TR = .675 sec), across nodes (x axis) as a function of window size (40 to 100 sec length) using overlapping windows as in (a). (F) The distribution of flexibility values across nodes shows high spatial similarity (correlations; all $p < .0001$). For the analyses shown in (E) and (F), flexibility values were derived after repeating the modularity analyses 10 times and choosing the run yielding the highest modularity value Q (see Methods for details).

Discussion

The present study investigated the associations between different aspects of intrinsic functional brain connectivity dynamics and psychological resilience. More specifically, we aimed to explore whether a previously proposed negative association between psychological resilience and node flexibility as determined using resting state BOLD fMRI (Long et al., 2019) can be replicated based on resting-state BOLD fMRI measured with a higher temporal resolution (multiband BOLD sequence; TR = .675 sec) in an independent sample that is comparable in terms of sample size, age, and gender distribution. Additionally, we aimed at extending previous findings by including two further metrics of network dynamics, as well as two further questionnaires with slightly different theoretical conceptions of resilience. Correlation analyses were performed at the levels of the whole brain, resting state networks, and individual nodes, to enable an investigation on different topological scales.

Results did not support the previously proposed associations – neither between node flexibility and resilience, nor for (1) any other measure of network dynamics, (2) for down-sampled data (TR = 2.025 sec) comparable to the temporal resolution of the data in Long et al. (2019), (3) for an analysis with non-overlapping time windows as implemented by Long et al. (2019), or (4) time windows of varying length between 40 and 100 sec. In the following, we will first discuss potential limitations of the present study, which may be important when considering reasons for the difference between the present and previous results. We will then discuss in more depth factors that may account for the failed replication of the results of Long et al. (2019).

Potential Limitations

In the present study, we used only one parcellation scheme, an atlas with 100 regions of interest by Schaefer and colleagues (Schaefer et al., 2018). The motivation for this was threefold: The findings of Long et al. (2019) were robust to changes in parcellation, as these authors replicated their effect (originally obtained using the AAL parcellation with 90 regions; (Tzourio-Mazoyer et al., 2002) using the Power atlas with 264 regions (Power et al., 2011). Secondly, recent evidence implies that functionally derived parcellations (as in the Schaefer atlas) outperform anatomical atlases like the AAL (Dadi et al., 2019). Lastly, given that our data had a higher temporal resolution, more fine-grained anatomical parcellations would have increased the computational demands of our study too much.

Furthermore, we chose the window size in accordance with the rule that it should be equal to $1/f_{min}$ (Leonardi & Van De Ville, 2015). This suggestion is motivated by the fact that due to their higher temporal resolution, MB-sequences might be prone to lower signal-to-noise ratio SNR caused by noise amplification (Risk et al., 2021). However, we cannot rule out that such long window sizes might hamper the sensitivity to small changes, as calculating connectivity matrices over longer periods serves as a smoothing kernel minimizing the ability to resolve TVFC (Vergara et al., 2019). However, this disadvantage of MB-EPI is more than compensated by the ability to acquire more data in the same time, the possibility to investigate faster dynamics, and to thus better disentangle neural and physiological signals (Yang & Lewis, 2021). Furthermore, we showed empirically for the present data that node flexibility was largely robust against changes in window size.

Potential limitations may also stem from the questionnaires used to assess resilience: Short versions of two scales (CD-RISC: 10 items, RS: 13 items) were used due to timing constraints, whereas the long (25-items) version of the CD-RISC was used by Long et al. (2019). However, we deem this unproblematic as validity studies show that also the short versions can be considered valid and reliable instruments for measuring trait resilience (Chmitorz et al., 2018; Leppert et al., 2008; Sarubin et al., 2015). This could also be confirmed based on our data, as all questionnaires showed satisfying levels of internal consistency.

Methodological considerations

Even though the overall direction of the correlation between node flexibility and resilience was the same in two previous publications using fMRI (Long et al., 2019) and EEG (Paban et al., 2019), the neural localizations of these correlations partly differed. Given this heterogeneity and the absence of such effects in our data, we refrain from discussing possible roles of specific brain regions or networks for resilience, but rather focus on specific methodological factors that may have contributed to the difference between our results and previous results.

Physiological Noise and Preprocessing. In conventional fMRI (TR = 2 sec) physiological signals often alias into the frequency range of interest, making it difficult to disentangle neural signal from noise. In contrast, the use of MB-sequences allows to better resolve the physiological signals in their respective frequency bands. This, in turn, allows for a better control of physiological noise (Risk et al., 2021; Yang & Lewis, 2021). However, we cannot draw a firm conclusion about possible differential influences of motion and noise on the results of our study vs. those of Long et al. (2019). Nevertheless, noise artifacts and their proper control are critical when calculating correlations between (TV)FC and behavioral measures (e.g., Siegel et al., 2017). For this reason, we have aimed to incorporate the most recent empirical insights regarding denoising strategies for module detection (Lydon-Staley et al., 2018) and imposed a strict FD-based cutoff to mitigate the impact of motion, which may have contributed to differences between our results and those of Long and colleagues (2019), who used fewer regressors for denoising.

Sliding Window Technique. We used an overlapping sliding window approach (length = 100s; step size = 1TR), which together with the MB-sequence allowed us to include 753 windows for TVFC analyses. This is the most distinct deviation as Long et al. (2019) used 12 non-overlapping windows (length= 40 sec). Both windowing schemes are among the most-used approaches within the sliding window framework (Iraji et al., 2020). For window-based TVFC analyses, the window length is a critical aspect, as it has to balance the ability of robustly estimating TVFC (which benefits from higher numbers of timepoints) against susceptibility to noise (Damaraju et al., 2020; Iraji et al., 2020). Extensive studies have evaluated the impact of different window types, lengths, and overlap on TVFC, however without yet identifying a gold standard (e.g.,

Abrol et al., 2017; Shakil et al., 2016). At present, lengths between 30s and 100s are commonly used (see Figure S1 in Preti et al., 2017). Within this set of possible parameter choices, one would however assume that strong effects should be robust against specific analysis choices (compare, e.g., Damaraju et al., 2020 vs. Haimovici et al., 2017). In accordance with this, our results did not vary between different temporal resolutions, windowing schemes, or window-sizes.

Reliability. Recent research suggests that multilayer modularity in particular (Yang et al., 2021) and TVFC in general (Hindriks et al., 2016) are a function of scanning duration and that rs-fMRI sequences around 10 min (as used by Long et al., 2019) are not sufficient for reliable parameter estimation. As reliability strongly influences which correlations are detectable (Hedge et al., 2018), short measurements may be prone to false positive correlations. Yang et al. (2021) propose that at least 20 min of rs-fMRI is needed for reliable multilayer modularity analysis - in that study based on a TR of 1.45 sec and non-overlapping windows of size 100 sec. In the present study, we measured 10 minutes of rs-fMRI with a TR of about half that length (as well as a substantially larger number of windows), intentionally selected to allow for reliable multilayer analyses. Yang et al. (2021) also suggest that the standard settings for intra- and interlayer parameters ($\gamma = \omega = 1$) in dynamic network measures may not necessarily turn out to be optimal across datasets and different network measures in terms of reliability. However, we deemed it problematic to tune these parameters independently for each network measure of interest (here: flexibility vs. promiscuity), as results would inevitably rely on different module structures which would introduce unsystematic variation and thereby weaken interpretability and comparability between measures. Consequently, we decided to replicate Long et al. (2019) as closely as possible and used the standard parameter settings of $\gamma = \omega = 1$.

Moreover, it is important that the behavioral variable of interest shows sufficient psychometric properties. The internal consistencies for our three resilience questionnaires were satisfactory, ranging from .70 to .85. Also, when investigating individual differences, samples should not be too homogeneous on the target measures, as inter-person variability is a precondition for detecting correlations. Even though CD-RISC data appear to be in a somewhat narrower range and more left-skewed than in Long et al. (2019), ranging from 18-38 (possible range 0-40), both the

RS-13 and the BRS show sufficient variability (RS-13: 21-87, possible range: 13-91; BRS: 1.83-5.00, possible range: 1-5), which increases confidence that our results are not solely driven by a lack of heterogeneity. Moreover, our sample showed scores comparable to the respective original publications. It is however difficult to compare our results directly to the studies by Paban et al. (2019) and Long et al. (2019) as the former did not report descriptive values (but high internal consistency: Cronbachs α = .90), whereas the latter did not report psychometrics but descriptive statistics.

Conclusion

To summarize, our results are not compatible with the previously suggested association between dynamical properties of the functional connectome and psychological resilience. We extended previous studies by including additional network measures and two further resilience questionnaires, and found no evidence of a correlation between dynamic network properties and self-reported resilience. Our study highlights and discusses the high degrees of freedom in the analysis of TVFC and brain networks, and consequently also underscores the need for testing the robustness and generalizability of proposed effects via replication.

Methods

Code and data have been deposited at https://zenodo.org/ under the doi:10.5281/zenodo.5113574 and will be made publicly available after an embargo period that ends December 31, 2024.

Participants

In total, N = 69 right-handed University students were enrolled in the study, of whom N = 60 completed the study procedure and were included for further analyses. All participants were native speakers of German, right handed, and between 18 and 35 years old; absence of current psychiatric episode was assured with a structured interview (MINI; Sheehan et al., 1998). This sample size was pre-registered based on calculations of statistical power for an analysis of BOLD activation differences between three tasks testing different facets of psychological flexibility (see https://osf.io/a64jn); the task-free (resting state) fMRI data reported here were acquired together with the pre-registered task-based fMRI experiments. During image quality checks and pre-

processing, eight datasets were excluded from further analyses (four due to low quality of questionnaire data and four due to motion artifact; see below for details of exclusion criteria), so that the reported analyses are based on data from 52 participants (26 females, 25 males, 1 diverse; 18-34 years; mean age 24.0 ± 3.7). All participants provided written informed consent and all procedures were approved by the Ethics Committee of the Department of Psychology of Goethe University Frankfurt, Germany.

Functional MR Image Acquisition

Resting state functional MRI (rsfMRI) data were collected prior to task-based fMRI (which is not part of the present report; see previous paragraph) on a 3-T Siemens Prisma MR-Scanner equipped with a 32-channel head coil, using a multiband (MB-factor = 4) echo planar imaging (EPI) sequence with the following parameters: 900 volumes (10:14 min), TR = 675 ms, TE = 30 ms, voxel size = 3 mm^3, flip angle = 60°, FoV = 222 mm, acquisition matrix = 74x74, 40 slices. During the rsfMRI measurement, participants were asked to keep their eyes open and gaze at a white fixation cross, located at the center of a screen (NNL; Nordic Neuro Lab, 40'', 1920x1080, 60Hz), to stay relaxed and not to think about anything specific. In a separate session, a T1 weighted (T1w) 3D structural MR scan was acquired with a MPRAGE sequence (4:26 min, voxelsize = 1 mm^3, TR = 1900 ms, TE = 2.52 ms, acquisition matrix = 256x256, 192 slices) for purposes of co-registration between functional and structural data.

Resilience Questionnaires

The psychological construct 'resilience' was quantified using German versions of three self-report questionnaires, the 10 item version of the Connor-Davidson Resilience Scale (CD-RISC – 10 items; Connor & Davidson, 2003; German version by Sarubin et al., 2015), the Brief Resilience Scale BRS – 6 items (Smith et al., 2008; German version by Chmitorz et al., 2018), and the Resilience Scale (RS – 13 items; Wagnild & Young, 1993; German version by Leppert et al., 2008). Note that short versions of the questionnaires were selected, as the present study was part of a more extensive study protocol and the short-version have been shown to allow for a time-efficient data collection with comparable validity and reliability (Chmitorz et al., 2018; Leppert et al., 2008; Sarubin et al., 2015). We included the CD-RISC and BRS because of their good ratings in an evaluation study by Windle and colleagues (2011). The RS was additionally chosen to increase comparability with other research, as this questionnaire

is frequently used in resilience research. In addition, the selected questionnaires also differ in that CD-RISC and RS define resilience as a personality trait, whereas resilience is understood as an outcome in the BRS (see original publications for more details).

Resilience questionnaires were filled out during an informational preparation session for the fMRI measurements and administered online using Unipark software (EFS Survey, Questback GmbH). As completion time of online questionnaires has been identified as the most reliable indicator of data being meaningful or meaningless (Leiner, 2013), we evaluated the quality of questionnaire data using a quality index provided by the Unipark system that compares the completion time of each participant with the average completion time of our sample. As preregistered (https://osf.io/c94y8) participants with an Unipark quality index of .20 or lower were excluded, resulting in exclusion of five participants (see also Leiner, 2013 for a similar criterion). Resilience scores were calculated according to the respective manuals. For each resilience scale, we also assessed internal consistency by calculating Cronbach's alpha and its 95% confidence interval (CI).

MR Data Quality Control

Quality of imaging data was assessed using both fMRIPREP´s visual reports as well as MRIQC 0.15.2rc1 (Esteban et al., 2017, 2019). T1w and functional images for each participant were visually checked for signal artifacts, whole brain coverage, and correct alignment between structural and functional data. Following a procedure proposed by Faskowitz and colleagues (2019) functional data were excluded if marked as an outlier (i.e., exceeding 1.5 x the inter-quartile-range either from Q1 or Q3) in more than 50% of the MRIQC quality metrics: *dvars, tsnr, snr, efc, aor, aqi* (see the MRIQC documentation, (Esteban et al., 2017), for more information about these metrics). Given the sensitivity of resting state analyses to movements and given that some of the aforementioned metrics are influenced by motion, we additionally included framewise displacement (FD) as a metric for quantifying motion artifacts (Maknojia et al., 2019). Due to the higher sampling rate of multiband EPI, motion parameters exhibit a high frequency (HF) component resulting from head motion due to respiration (Power et al., 2019) that is usually not observable with standard single-band fMRI (Williams & Van Snellenberg, 2019). With this 'spurious' HF motion component, the head appears to be in constant motion and summary measures (such as FD) might be contaminated,

leading to exaggerated flagging of 'bad' volumes. Note that this applies less to subsequent functional connectivity measures, as those are routinely band-pass filtered, whereas summary measures (e.g., FD) are calculated on raw motion parameters (Gratton et al., 2020; Power et al., 2019; Williams & Van Snellenberg, 2019). We therefore calculated filtered FD (FD_{filt}) from Butterworth-filtered raw head movement traces to better isolate 'true' head movements (Power et al., 2019). Following Lydon-Staley et al. (2018), we excluded subjects with mean FD_{filt} >0.2 mm or >20 volumes with FD_{filt} >0.25 mm to ensure high data quality. We excluded four subjects based on their FD_{filt}, while no subject was excluded based on MRIQC´s metrics.

Image Preprocessing

T1w and rfMRI images were preprocessed using *fMRIPREP* 20.1.1 (Esteban et al., 2019) which is based on Nipype 1.5.0 (Gorgolewski et al., 2011). A boilerplate text released under a CC0 license describing preprocessing details can be found in the Supplementary File 1. For further pipeline information, see fMRIPREP´s documentation (Esteban et al., 2019). Due to the use of MB data and the high sampling rate, no slice time correction was applied (see e.g., Glasser et al., 2013). Distortion corrected functional images in T1w space were further denoised using the XPC Engine 1.2.1 (Ciric et al., 2017). We implemented a denoising strategy that has been shown to be relatively effective in mitigating motion artifacts in the study of dynamic functional connectivity, (multilayer) subnetwork detection and measures of module reconfiguration (Lydon-Staley et al., 2018). BOLD data was first demeaned, detrended, and despiked on a voxelwise basis (instead of using more aggressive censoring methods that may result in varying window lengths across participants; (Hutchison et al., 2013) and then temporally filtered with a first-order Butterworth-filter using a passband of 0.01 – 0.08 Hz. These operations were followed by a confound regression, that included (1) six motion estimates derived from fMRIPREPs realignment, (2) mean signals from white matter (WM) and cerebrospinal fluid (CSF), (3) mean global signal, (4) temporal derivatives of these 9 regressors, as well as (5) the quadratic terms of all 18 parameters, resulting in a 36-parameter model to obtain residual BOLD time series. All regressors were also bandpass filtered to avoid reintroducing noise caused by a frequency-dependent mismatch (Hallquist et al., 2013). Within the XCP engine, the Schaefer parcellation (Schaefer et al., 2018) was

transformed to native T1 space and resampled to match the BOLD images. For each subject the whole brain was parcellated into 100 regions (which can be grouped to match the seven functional networks described by Yeo et al. (2011) and a functional time series was extracted for each region, corresponding to the average across all voxels within that region.

Time Varying Functional Connectivity (TVFC)

All subsequent TVFC analyses were performed with the numpy (1.18.5; Harris et al., 2020) and scipy (1.5.0, SciPy 1.0 Contributors et al., 2020) package in python 3.8.3. We used a sliding window approach with a fixed window length of 148 time-points (= 100 sec), that (1) satisfies the frequency criterion that the length should be at least be equal to $1/f_{min}$ (Leonardi & Van De Ville, 2015) and (2) allows for a full oscillation of the slowest frequency in the range of 0.01 - 0.08Hz. Windows were shifted by a single timepoint (TR) and tapered with a Hamming filter to reduce potential edge artifacts and suppress spurious correlations (Shakil et al., 2016; Zalesky et al., 2014). Pairwise Pearson correlation coefficients between all nodes were calculated within each window, yielding 753 connectivity matrices per subject.

We calculated the standard deviation (SD) of each node x node correlation (i.e., node-node connection or edge) over time as a proxy for TVFC (often also referred to as 'dynamic' connectivity; Lurie et al., 2020). To test whether these SDs likely reflect 'true' dynamics, we benchmarked these estimates against phase randomized surrogate (null) data that preserved auto-correlation, power spectral density and stationary cross correlation of the observed data (Lurie et al., 2020; Prichard & Theiler, 1994; Savva et al., 2019). More precisely, we created 500 surrogates for each subject by phase randomizing the empirical timeseries obtained from the 100 nodes. To preserve the correlative structure between node timeseries, all signals were multiplied by the same uniformly random phase and the SD for each edge was calculated, respectively (see Savva et al., 2019 for a detailed description of phase randomization). The empirically observed SDs were ranked against this null distribution and *p*-values were obtained by dividing the number of times $SD_{surr} >= SD_{real}$ by the number of surrogates. Given that each subject has 4,950 unique connections, FDR-correction ($p < 0.05$) was applied to reduce type-I-errors.

To describe ‘dynamics’ in nodal space, we calculated the nodal degree metric as the binary sum of significant (i.e., ‘dynamic’) connections for each node (Pedersen et al., 2018). Of note, when testing TVFC with surrogate null data, one needs to be cautious as the absence of significance (relative to the null model) does not necessarily indicate the absence of dynamic connectivity. This interpretation depends heavily on the null model applied, and the data may contain meaningful fluctuations relative to other definitions of the null model (see Lurie et al., 2020 for a comprehensive overview).

Multilayer Modularity

For multilayer modularity, negative correlations in each node x node matrix (i.e., per subject and time window) were set to zero and correlations were z-transformed as done in previous studies (e.g., Finc et al., 2020; Pedersen et al., 2018). We constructed an ordinal multilayer network in which each layer (i.e., time window) represents a weighted adjacency matrix. To assess the spatiotemporal community structure and to track network reconfigurations, each node was linked to itself across layers. To detect communities (i.e., groups of nodes that are more densely connected to one another than to the rest of the network), we used the multilayer counterpart (Mucha et al., 2010) of the modularity function proposed by Newman and Girvan (2004).

In general, community detection and node assignment can be solved algorithmically by maximizing the modularity quality function Q. Q allows to quantify the goodness of fit of a certain partition, with high values indicating high quality partitions (Furtunato, 2010). Following the idea that random graphs do not show a cluster structure, the quality function compares the number of intracommunity edges to what would be expected at random (i.e., under a null model), to quantify communities (Fortunato, 2010; Mucha et al., 2010). The quality function Q can be formalized as follows:

$$Q = \sum_{ij} \left(A_{ij} - P_{ij}\right) \delta\left(M_i, M_j\right) \quad (1)$$

where A_{ij} and P_{ij} are the observed and expected weights of the connection between node *i* and node *j*. Here, A_{ij} is an element of the adjacency matrix $\mathbf{A}$ and P_{ij} refers to a specific null model. The Kronecker delta function $\delta\left(M_i, M_j\right)$ equals 1 if node *i* and *j* are assigned to the same module (M) and 0 if otherwise. Noteworthy, the modularity function suffers from a “resolution limit”, meaning that communities that are rather

small compared to the whole graph may be undetectable (Fortunato & Barthelemy, 2007). To overcome this caveat, one may introduce a structural resolution parameter γ that weights the null model. Optimizing $Q(\gamma)$ with large values of γ leads to the detection of many small communities, whereas small values of γ result in few large communities. Here, we used an expanded modularity function that can be used with multilayer networks, formalized as follows:

$$Q(\gamma,\omega) = \frac{1}{2\mu}\sum_{ijsr}\left[\left(A_{ijs} - \gamma_s \frac{k_{is}k_{js}}{2m_s}\right)\delta(M_{is},M_{js}) + \delta_{ij}\,\omega_{jsr}\right]\delta(M_{is},M_{jr}) \quad (2)$$

where A_{ijs} describes elements of $\mathbf{A}$ of layer (time window) s and $\frac{k_{is}k_{js}}{2m_s}$ denotes the Newman-Girvan configuration null model (i.e., the expected connectivity strength at chance level, with k = node degree at layer s; m = sum of all edges at layer s) that is scaled by the resolution parameter γ_s of layer s, $\delta(M_{is},M_{js})$ and $\delta(M_{is},M_{jr})$ = 1 if node *i* and node *j* are in the same module (M) or 0 if they do not belong to the same module (here M_{is} depicts the community assignment of node *i* in layer *s*; ω_{jsr} is the interlayer coupling parameter connecting node *j* in layer s to itself in layer r, defining the similarity of communities across layers with large values of ω_{jsr} leading to increased homogeneity across layers, as nodes will prefer to stay in one community (Vaiana & Muldoon, 2018). To optimize the multilayer modularity function, we used an iterative and generative Louvain like algorithm implemented with code from
Lucas G. S. Jeub, Marya Bazzi, Inderjit S. Jutla, and Peter J. Mucha, [*"A generalized Louvain method for community detection implemented in MATLAB,"* https://github.com/GenLouvain/GenLouvain (2011-2019)]. The tunable parameters γ and ω were held constant across layers and set to unity, as had been done in previous studies (e.g., Braun et al., 2015; Yin et al., 2020). As the modularity approach is not deterministic, we repeated it 100 times for each participant and chose the run yielding the highest modularity value, as e.g., done in Finc et al. (2020).

Time Resolved Analyses of Brain Network Reconfiguration

Within the time-varying community framework, we assessed *node flexibility* as the number of times a node changes its community assignment between adjacent layers, normalized by the total number of possible changes. Node flexibility can be interpreted as a metric that allows to quantify reconfigurations of functional connectivity patterns

that a brain region undergoes over time (Braun et al., 2015). To enrich the spatiotemporal description of a node, we further calculated *node promiscuity*, defined as the fraction of communities a node participates in at least once, across all layers. This metric allows to quantify the distribution of a node`s connections over time, e.g., whether high flexibility stems from a switching between two communities or an evenly distributed allegiance to a larger number of different modules (Garcia et al., 2018; Papadopoulos et al., 2016). The higher the nodal promiscuity, the more modules a node participates at least once across time.

For each of the three node-specific measures of dynamic network reconfiguration, i.e., flexibility, promiscuity, and degree, we additionally calculated the respective global measure (e.g., global flexibility) as the average measure across all nodes, as well as seven network-specific measures by averaging across all nodes belonging to the respective resting-state networks (RSNs) as proposed by Yeo and colleagues (2011), i.e., visual, somatomotor, dorsal attention, ventral attention (salience), limbic, fronto-parietal control, default mode.

Control Analyses

Down-Sampling. To better compare our results to the findings described in Long et. al (2019) and to investigate if different sampling rates or window schemes (i.e., MB-EPI vs conventional EPI) yield different results, we down-sampled our original resting state BOLD timeseries in a second step by a factor of three to resemble a TR of 2 as closely as possible (given that 3 x .675 sec = 2.025 sec). Raw motion traces were also down-sampled accordingly, and FD was calculated without filtering. Sliding window correlations with an adjusted window length of 50 timepoints (= 101.25 s) and subsequent TVFC and modularity analyses were calculated as described above. Furthermore, we segmented the time series into 15 non-overlapping windows with length of 20 TR, i.e., a length of 40,5 sec, analogous to the windowing scheme used in Long et al., 2019). To investigate whether the calculated network measures differ between original and down-sampled data and to rule out any idiosyncratic algorithmic behavior (i.e., from multilayer modularity), we compared all three metrics on a nodal level, as these were the starting points for all subsequent measures. For node flexibility and node promiscuity we calculated the spatial similarity (i.e., Spearman correlation coefficient) between mean values per node (average over participants) in the original and down-sampled data, to explore whether nodes behave in comparable manner in

both time series. As the down-sampling creates 'sparser' data and disrupts the smoothness of the original data (which might result in more abrupt changes in community-assignments), we anticipated a tendency towards higher values for both metrics in the down-sampled data. For node degree, we expected lower values in the down-sampled data, as a recent study by Pedersen et al. (2018) showed that nodal degree decreased with less available data and thus tested this hypothesis using a paired t-test.

Window Length. Given that window sizes in the range of 30 to 100 sec are widely used across studies (Preti et al., 2017), we additionally tested the influence of varying window sizes, i.e., between 40 and 80 sec in steps of 20, on node flexibility, and their effects on the correlation with psychological resilience.

Correlation Analyses

All subsequent analyses were performed with the pingouin statistics package (0.3.11; Vallat, 2018) in python 3.8.3. To test for associations between resilience and time-varying brain network measures, we calculated partial (Spearman) correlations with age, gender, and FD included as covariates of no interest to resemble the study by Long and colleagues (2019). Note that unlike Long et al. (2019), years of education was not included as covariate, as all participants were students and we thus had not acquired years of education in our study. Correlations were performed at the global, nodal, and network-specific levels for all pairwise combinations between resilience questionnaires (CDRISC, BRS, RS), network measures (flexibility, promiscuity, degree), and for original vs down-sampled data as well as for varying windowing schemes (see previous section). Results were corrected for multiple statistical comparisons using the false discovery rate ($p < .05$; Benjamini & Hochberg, 1995). To investigate whether null results were driven by the inclusion of covariates, we additionally re-calculated all pairwise correlations (nodal level) without covariates.

Author Contributions

Conceptualization: D.K., C.J.F.

Software: D.K.

Project administration: D.K., C.J.F.

Investigation: D.K.

Data curation: D.K.

Formal analysis: D.K.

Visualization: D.K.

Writing – original draft: D.K., C.J.F.

Writing – review & editing: D.K., C.J.F.

Funding Information

This research was funded by the German Research Foundation (CRC 1193 grant no. INST 247/859-1 awarded to C.J.F.). D.K. is supported by the German Academic Scholarship Foundation.

Acknowledgments

We would like to thank Dr. Cindy Eckart for providing valuable comments on an earlier version of this manuscript and our research assistants for their help in data collection.

References

Abrol, A., Damaraju, E., Miller, R. L., Stephen, J. M., Claus, E. D., Mayer, A. R., & Calhoun, V. D. (2017). Replicability of time-varying connectivity patterns in large resting state fMRI samples. *NeuroImage*, *163*, 160–176. https://doi.org/10.1016/j.neuroimage.2017.09.020

Bassett, D. S., Wymbs, N. F., Porter, M. A., Mucha, P. J., Carlson, J. M., & Grafton, S. T. (2011). Dynamic reconfiguration of human brain networks during learning. *Proceedings of the National Academy of Sciences*, *108*(18), 7641–7646. https://doi.org/10.1073/pnas.1018985108

Benjamini, Y., & Hochberg, Y. (1995). Controlling the False Discovery Rate: A Practical and Powerful Approach to Multiple Testing. *Journal of the Royal Statistical Society. Series B (Methodological)*, *57*(1), 289–300.

Braun, U., Schäfer, A., Walter, H., Erk, S., Romanczuk-Seiferth, N., Haddad, L., Schweiger, J. I., Grimm, O., Heinz, A., Tost, H., Meyer-Lindenberg, A., & Bassett, D. S. (2015). Dynamic reconfiguration of frontal brain networks during executive cognition in humans. *Proceedings of the National Academy of Sciences*, *112*(37), 11678–11683. https://doi.org/10.1073/pnas.1422487112

Chmitorz, A., Wenzel, M., Stieglitz, R.-D., Kunzler, A., Bagusat, C., Helmreich, I., Gerlicher, A., Kampa, M., Kubiak, T., Kalisch, R., Lieb, K., & Tüscher, O. (2018). Population-based validation of a German version of the Brief Resilience Scale. *PLOS ONE*, *13*(2), e0192761. https://doi.org/10.1371/journal.pone.0192761

Ciric, R., Wolf, D. H., Power, J. D., Roalf, D. R., Baum, G. L., Ruparel, K., Shinohara, R. T., Elliott, M. A., Eickhoff, S. B., Davatzikos, C., Gur, R. C., Gur, R. E., Bassett, D. S., & Satterthwaite, T. D. (2017). Benchmarking of participant-level confound regression strategies for the control of motion artifact in studies of functional connectivity. *NeuroImage*, *154*, 174–187. https://doi.org/10.1016/j.neuroimage.2017.03.020

Connor, K. M., & Davidson, J. R. T. (2003). Development of a new resilience scale: The Connor-Davidson Resilience Scale (CD-RISC). *Depression and Anxiety*, *18*(2), 76–82. https://doi.org/10.1002/da.10113

Dadi, K., Rahim, M., Abraham, A., Chyzhyk, D., Milham, M., Thirion, B., & Varoquaux, G. (2019). Benchmarking functional connectome-based predictive

models for resting-state fMRI. *NeuroImage*, *192*, 115–134. https://doi.org/10.1016/j.neuroimage.2019.02.062

Damaraju, E., Tagliazucchi, E., Laufs, H., & Calhoun, V. D. (2020). Connectivity dynamics from wakefulness to sleep. *NeuroImage*, *220*, 117047. https://doi.org/10.1016/j.neuroimage.2020.117047

Dong, D., Wang, Y., Chang, X., Luo, C., & Yao, D. (2018). Dysfunction of Large-Scale Brain Networks in Schizophrenia: A Meta-analysis of Resting-State Functional Connectivity. *Schizophrenia Bulletin*, *44*(1), 168–181. https://doi.org/10.1093/schbul/sbx034

Esteban, O., Birman, D., Schaer, M., Koyejo, O. O., Poldrack, R. A., & Gorgolewski, K. J. (2017). MRIQC: Advancing the automatic prediction of image quality in MRI from unseen sites. *PLoS ONE*, *12*(9). https://doi.org/10.1371/journal.pone.0184661

Esteban, O., Markiewicz, C. J., Blair, R. W., Moodie, C. A., Isik, A. I., Erramuzpe, A., Kent, J. D., Goncalves, M., DuPre, E., Snyder, M., Oya, H., Ghosh, S. S., Wright, J., Durnez, J., Poldrack, R. A., & Gorgolewski, K. J. (2019). fMRIPrep: A robust preprocessing pipeline for functional MRI. *Nature Methods*, *16*(1), 111–116. https://doi.org/10.1038/s41592-018-0235-4

Faskowitz, J., Esfahlani, F. Z., Jo, Y., Sporns, O., & Betzel, R. F. (2019). Edge-centric functional network representations of human cerebral cortex reveal overlapping system-level architecture. *BioRxiv*, 799924. https://doi.org/10.1101/799924

Finc, K., Bonna, K., He, X., Lydon-Staley, D. M., Kühn, S., Duch, W., & Bassett, D. S. (2020). Dynamic reconfiguration of functional brain networks during working memory training. *Nature Communications*, *11*(1), 2435. https://doi.org/10.1038/s41467-020-15631-z

Fortunato, S., & Barthelemy, M. (2007). Resolution limit in community detection. *Proceedings of the National Academy of Sciences*, *104*(1), 36–41. https://doi.org/10.1073/pnas.0605965104

Furtunato, S. (2010). Community detection in graphs. *Physics Reports*, *486*(3–5), 75–174. https://doi.org/10.1016/j.physrep.2009.11.002

Garcia, J. O., Ashourvan, A., Muldoon, S. F., Vettel, J. M., & Bassett, D. S. (2018). Applications of community detection techniques to brain graphs: Algorithmic considerations and implications for neural function. *Proceedings of the IEEE.*

Institute of Electrical and Electronics Engineers, *106*(5), 846–867. https://doi.org/10.1109/JPROC.2017.2786710

Glasser, M. F., Sotiropoulos, S. N., Wilson, J. A., Coalson, T. S., Fischl, B., Andersson, J. L., Xu, J., Jbabdi, S., Webster, M., Polimeni, J. R., Van Essen, D. C., & Jenkinson, M. (2013). The Minimal Preprocessing Pipelines for the Human Connectome Project. *NeuroImage*, *80*, 105–124. https://doi.org/10.1016/j.neuroimage.2013.04.127

Gorgolewski, K., Burns, C. D., Madison, C., Clark, D., Halchenko, Y. O., Waskom, M. L., & Ghosh, S. S. (2011). Nipype: A Flexible, Lightweight and Extensible Neuroimaging Data Processing Framework in Python. *Frontiers in Neuroinformatics*, *5*. https://doi.org/10.3389/fninf.2011.00013

Gratton, C., Dworetsky, A., Coalson, R. S., Adeyemo, B., Laumann, T. O., Wig, G. S., Kong, T. S., Gratton, G., Fabiani, M., Barch, D. M., Tranel, D., Miranda-Dominguez, O., Fair, D. A., Dosenbach, N. U. F., Snyder, A. Z., Perlmutter, J. S., Petersen, S. E., & Campbell, M. C. (2020). Removal of high frequency contamination from motion estimates in single-band fMRI saves data without biasing functional connectivity. *bioRxiv*, 837161. https://doi.org/10.1101/837161

Haimovici, A., Tagliazucchi, E., Balenzuela, P., & Laufs, H. (2017). On wakefulness fluctuations as a source of BOLD functional connectivity dynamics. *Scientific Reports*, *7*(1), 5908. https://doi.org/10.1038/s41598-017-06389-4

Hallquist, M. N., Hwang, K., & Luna, B. (2013). The nuisance of nuisance regression: Spectral misspecification in a common approach to resting-state fMRI preprocessing reintroduces noise and obscures functional connectivity. *NeuroImage*, *82*, 208–225. https://doi.org/10.1016/j.neuroimage.2013.05.116

Harris, C. R., Millman, K. J., van der Walt, S. J., Gommers, R., Virtanen, P., Cournapeau, D., Wieser, E., Taylor, J., Berg, S., Smith, N. J., Kern, R., Picus, M., Hoyer, S., van Kerkwijk, M. H., Brett, M., Haldane, A., del Río, J. F., Wiebe, M., Peterson, P., … Oliphant, T. E. (2020). Array programming with NumPy. *Nature*, *585*(7825), 357–362. https://doi.org/10.1038/s41586-020-2649-2

Hedge, C., Powell, G., & Sumner, P. (2018). The reliability paradox: Why robust cognitive tasks do not produce reliable individual differences. *Behavior Research Methods*, *50*(3), 1166–1186. https://doi.org/10.3758/s13428-017-

0935-1

Hindriks, R., Adhikari, M. H., Murayama, Y., Ganzetti, M., Mantini, D., Logothetis, N. K., & Deco, G. (2016). Can sliding-window correlations reveal dynamic functional connectivity in resting-state fMRI? *NeuroImage*, *127*, 242–256. https://doi.org/10.1016/j.neuroimage.2015.11.055

Hutchison, R. M., Womelsdorf, T., Allen, E. A., Bandettini, P. A., Calhoun, V. D., Corbetta, M., Della Penna, S., Duyn, J. H., Glover, G. H., Gonzalez-Castillo, J., Handwerker, D. A., Keilholz, S., Kiviniemi, V., Leopold, D. A., de Pasquale, F., Sporns, O., Walter, M., & Chang, C. (2013). Dynamic functional connectivity: Promise, issues, and interpretations. *NeuroImage*, *80*, 360–378. https://doi.org/10.1016/j.neuroimage.2013.05.079

Iraji, A., Faghiri, A., Lewis, N., Fu, Z., Rachakonda, S., & Calhoun, V. D. (2020). Tools of the trade: Estimating time-varying connectivity patterns from fMRI data. *Social Cognitive and Affective Neuroscience*, *nsaa114*. https://doi.org/10.1093/scan/nsaa114

Leiner, D. J. (2013). Too Fast, Too Straight, Too Weird: Post Hoc Identification of Meaningless Data in Internet Surveys. *SSRN Electronic Journal*. https://doi.org/10.2139/ssrn.2361661

Leonardi, N., & Van De Ville, D. (2015). On spurious and real fluctuations of dynamic functional connectivity during rest. *NeuroImage*, *104*, 430–436. https://doi.org/10.1016/j.neuroimage.2014.09.007

Leppert, K., Koch, B., Brähler, E., & Strauß, B. (2008). *Die Resilienzskala (RS) – Überprüfung der Langform RS-25 und einer Kurzform RS-13*.

Li, S., Hu, N., Zhang, W., Tao, B., Dai, J., Gong, Y., Tan, Y., Cai, D., & Lui, S. (2019). Dysconnectivity of Multiple Brain Networks in Schizophrenia: A Meta-Analysis of Resting-State Functional Connectivity. *Frontiers in Psychiatry*, *10*, 482. https://doi.org/10.3389/fpsyt.2019.00482

Long, Y., Chen, C., Deng, M., Huang, X., Tan, W., Zhang, L., Fan, Z., & Liu, Z. (2019). Psychological resilience negatively correlates with resting-state brain network flexibility in young healthy adults: A dynamic functional magnetic resonance imaging study. *Annals of Translational Medicine*, *7*(24), 809. https://doi.org/10.21037/atm.2019.12.45

Lurie, D. J., Kessler, D., Bassett, D. S., Betzel, R. F., Breakspear, M., Kheilholz, S., Kucyi, A., Liégeois, R., Lindquist, M. A., McIntosh, A. R., Poldrack, R. A.,

Shine, J. M., Thompson, W. H., Bielczyk, N. Z., Douw, L., Kraft, D., Miller, R. L., Muthuraman, M., Pasquini, L., … Calhoun, V. D. (2020). Questions and controversies in the study of time-varying functional connectivity in resting fMRI. *Network Neuroscience*, *4*(1), 30–69. https://doi.org/10.1162/netn_a_00116

Lydon-Staley, D. M., Ciric, R., Satterthwaite, T. D., & Bassett, D. S. (2018). Evaluation of confound regression strategies for the mitigation of micromovement artifact in studies of dynamic resting-state functional connectivity and multilayer network modularity. *Network Neuroscience*, 1–28. https://doi.org/10.1162/netn_a_00071

Maknojia, S., Churchill, N. W., Schweizer, T. A., & Graham, S. J. (2019). Resting State fMRI: Going Through the Motions. *Frontiers in Neuroscience*, *13*, 825. https://doi.org/10.3389/fnins.2019.00825

Menon, V. (2011). Large-scale brain networks and psychopathology: A unifying triple network model. *Trends in Cognitive Sciences*, *15*(10), 483–506. https://doi.org/10.1016/j.tics.2011.08.003

Mucha, P. J., Richardson, T., Macon, K., Porter, M. A., & Onnela, J.-P. (2010). Community Structure in Time-Dependent, Multiscale, and Multiplex Networks. *Science*, *328*(5980), 876–878. https://doi.org/10.1126/science.1184819

Mulders, P. C., van Eijndhoven, P. F., Schene, A. H., Beckmann, C. F., & Tendolkar, I. (2015). Resting-state functional connectivity in major depressive disorder: A review. *Neuroscience & Biobehavioral Reviews*, *56*, 330–344. https://doi.org/10.1016/j.neubiorev.2015.07.014

Muldoon, S. F., & Bassett, D. S. (2016). Network and Multilayer Network Approaches to Understanding Human Brain Dynamics. *Philosophy of Science*, *83*(5), 710–720. https://doi.org/10.1086/687857

Newman, M. E. J., & Girvan, M. (2004). Finding and evaluating community structure in networks. *Physical Review E*, *69*(2), 026113. https://doi.org/10.1103/PhysRevE.69.026113

Paban, V., Modolo, J., Mheich, A., & Hassan, M. (2019). Psychological resilience correlates with EEG source-space brain network flexibility. *Network Neuroscience*, *3*(2), 539–550. https://doi.org/10.1162/netn_a_00079

Papadopoulos, L., Puckett, J. G., Daniels, K. E., & Bassett, D. S. (2016). Evolution of network architecture in a granular material under compression. *Physical*

Review. E, *94*(3–1), 032908. https://doi.org/10.1103/PhysRevE.94.032908

Pedersen, M., Zalesky, A., Omidvarnia, A., & Jackson, G. D. (2018). Multilayer network switching rate predicts brain performance. *Proceedings of the National Academy of Sciences*, *115*(52), 13376–13381. https://doi.org/10.1073/pnas.1814785115

Power, J. D., Cohen, A. L., Nelson, S. M., Wig, G. S., Barnes, K. A., Church, J. A., Vogel, A. C., Laumann, T. O., Miezin, F. M., Schlaggar, B. L., & Petersen, S. E. (2011). Functional network organization of the human brain. *Neuron*, *72*(4), 665–678. https://doi.org/10.1016/j.neuron.2011.09.006

Power, J. D., Lynch, C. J., Silver, B. M., Dubin, M. J., Martin, A., & Jones, R. M. (2019). Distinctions among real and apparent respiratory motions in human fMRI data. *NeuroImage*, *201*, 116041. https://doi.org/10.1016/j.neuroimage.2019.116041

Preti, M. G., Bolton, T. A., & Van De Ville, D. (2017). The dynamic functional connectome: State-of-the-art and perspectives. *NeuroImage*, *160*, 41–54. https://doi.org/10.1016/j.neuroimage.2016.12.061

Prichard, D., & Theiler, J. (1994). Generating surrogate data for time series with several simultaneously measured variables. *Physical Review Letters*, *73*(7), 951–954. https://doi.org/10.1103/PhysRevLett.73.951

Risk, B. B., Murden, R. J., Wu, J., Nebel, M. B., Venkataraman, A., Zhang, Z., & Qiu, D. (2021). Which multiband factor should you choose for your resting-state fMRI study? *NeuroImage*, *234*, 117965. https://doi.org/10.1016/j.neuroimage.2021.117965

Sarubin, N., Gutt, D., Giegling, I., Bühner, M., Hilbert, S., Krähenmann, O., Wolf, M., Jobst, A., Sabaß, L., Rujescu, D., Falkai, P., & Padberg, F. (2015). Erste Analyse der psychometrischen Eigenschaften und Struktur der deutschsprachigen 10- und 25-Item Version der Connor-Davidson Resilience Scale (CD-RISC). *Zeitschrift für Gesundheitspsychologie*, *23*(3), 112–122. https://doi.org/10.1026/0943-8149/a000142

Savva, A. D., Mitsis, G. D., & Matsopoulos, G. K. (2019). Assessment of dynamic functional connectivity in resting-state fMRI using the sliding window technique. *Brain and Behavior*, *9*(4), e01255. https://doi.org/10.1002/brb3.1255

Schaefer, A., Kong, R., Gordon, E. M., Laumann, T. O., Zuo, X.-N., Holmes, A. J.,

Eickhoff, S. B., & Yeo, B. T. T. (2018). Local-Global Parcellation of the Human Cerebral Cortex from Intrinsic Functional Connectivity MRI. *Cerebral Cortex (New York, N.Y.: 1991)*, *28*(9), 3095–3114. https://doi.org/10.1093/cercor/bhx179

SciPy 1.0 Contributors, Virtanen, P., Gommers, R., Oliphant, T. E., Haberland, M., Reddy, T., Cournapeau, D., Burovski, E., Peterson, P., Weckesser, W., Bright, J., van der Walt, S. J., Brett, M., Wilson, J., Millman, K. J., Mayorov, N., Nelson, A. R. J., Jones, E., Kern, R., … van Mulbregt, P. (2020). SciPy 1.0: Fundamental algorithms for scientific computing in Python. *Nature Methods*, *17*(3), 261–272. https://doi.org/10.1038/s41592-019-0686-2

Shakil, S., Lee, C.-H., & Keilholz, S. D. (2016). Evaluation of sliding window correlation performance for characterizing dynamic functional connectivity and brain states. *NeuroImage*, *133*, 111–128. https://doi.org/10.1016/j.neuroimage.2016.02.074

Sheehan, D. V., Lecrubier, Y., Sheehan, K. H., Amorim, P., Janavs, J., Weiller, E., Hergueta, T., Baker, R., & Dunbar, G. C. (1998). The Mini-International Neuropsychiatric Interview (M.I.N.I.): The development and validation of a structured diagnostic psychiatric interview for DSM-IV and ICD-10. *The Journal of Clinical Psychiatry*, *59 Suppl 20*, 22-33;quiz 34-57.

Siegel, J. S., Mitra, A., Laumann, T. O., Seitzman, B. A., Raichle, M., Corbetta, M., & Snyder, A. Z. (2017). Data Quality Influences Observed Links Between Functional Connectivity and Behavior. *Cerebral Cortex (New York, N.Y.: 1991)*, *27*(9), 4492–4502. https://doi.org/10.1093/cercor/bhw253

Smith, B. W., Dalen, J., Wiggins, K., Tooley, E., Christopher, P., & Bernard, J. (2008). The brief resilience scale: Assessing the ability to bounce back. *International Journal of Behavioral Medicine*, *15*(3), 194–200. https://doi.org/10.1080/10705500802222972

Southwick, S. M., & Charney, D. S. (2012). The Science of Resilience: Implications for the Prevention and Treatment of Depression. *Science*, *338*(6103), 79–82. https://doi.org/10.1126/science.1222942

Tzourio-Mazoyer, N., Landeau, B., Papathanassiou, D., Crivello, F., Etard, O., Delcroix, N., Mazoyer, B., & Joliot, M. (2002). Automated anatomical labeling of activations in SPM using a macroscopic anatomical parcellation of the MNI MRI single-subject brain. *NeuroImage*, *15*(1), 273–289.

https://doi.org/10.1006/nimg.2001.0978

Vaiana, M., & Muldoon, S. (2018). Resolution Limits for Detecting Community Changes in Multilayer Networks. *arXiv:1803.03597 [physics]*. http://arxiv.org/abs/1803.03597

Vallat, R. (2018). Pingouin: Statistics in Python. *Journal of Open Source Software*, *3*(31), 1026. https://doi.org/10.21105/joss.01026

Vergara, V. M., Abrol, A., & Calhoun, V. D. (2019). An average sliding window correlation method for dynamic functional connectivity. *Human Brain Mapping*, *40*(7), 2089–2103. https://doi.org/10.1002/hbm.24509

Wagnild, G. M., & Young, H. M. (1993). Development and psychometric evaluation of the Resilience Scale. *Journal of Nursing Measurement*, *1*(2), 165–178.

Williams, J. C., & Van Snellenberg, J. X. (2019). *Motion denoising of multiband resting state functional connectivity MRI data: An improved volume censoring method* [Preprint]. Neuroscience. https://doi.org/10.1101/860635

Windle, G., Bennett, K. M., & Noyes, J. (2011). A methodological review of resilience measurement scales. *Health and Quality of Life Outcomes*, *9*, 8. https://doi.org/10.1186/1477-7525-9-8

Yang, Z., & Lewis, L. D. (2021). Imaging the temporal dynamics of brain states with highly sampled fMRI. *Current Opinion in Behavioral Sciences*, *40*, 87–95. https://doi.org/10.1016/j.cobeha.2021.02.005

Yang, Z., Telesford, Q. K., Franco, A. R., Lim, R., Gu, S., Xu, T., Ai, L., Castellanos, F. X., Yan, C.-G., Colcombe, S., & Milham, M. P. (2021). Measurement reliability for individual differences in multilayer network dynamics: Cautions and considerations. *NeuroImage*, *225*, 117489. https://doi.org/10.1016/j.neuroimage.2020.117489

Yeo, B. T. T., Krienen, F. M., Sepulcre, J., Sabuncu, M. R., Lashkari, D., Hollinshead, M., Roffman, J. L., Smoller, J. W., Zöllei, L., Polimeni, J. R., Fischl, B., Liu, H., & Buckner, R. L. (2011). The organization of the human cerebral cortex estimated by intrinsic functional connectivity. *Journal of Neurophysiology*, *106*(3), 1125–1165. https://doi.org/10.1152/jn.00338.2011

Yin, W., Li, T., Hung, S.-C., Zhang, H., Wang, L., Shen, D., Zhu, H., Mucha, P. J., Cohen, J. R., & Lin, W. (2020). The emergence of a functionally flexible brain during early infancy. *Proceedings of the National Academy of Sciences*, 202002645. https://doi.org/10.1073/pnas.2002645117

Zalesky, A., Fornito, A., Cocchi, L., Gollo, L. L., & Breakspear, M. (2014). Time-resolved resting-state brain networks. *Proceedings of the National Academy of Sciences*, *111*(28), 10341–10346. https://doi.org/10.1073/pnas.1400181111